

# Photoemission spectra of LaMnO<sub>3</sub> controlled by orbital excitations

Jeroen van den Brink,<sup>1</sup> Peter Horsch,<sup>1</sup> and Andrzej M. Oleś<sup>2,1</sup>

<sup>1</sup>*Max-Planck-Institut für Festkörperforschung, Heisenbergstrasse 1, D-70569 Stuttgart, Germany*

<sup>2</sup>*Institute of Physics, Jagellonian University, Reymonta 4, PL-30059 Kraków, Poland*

(August 26, 2019)

We investigate the spectral function of a hole moving in the orbital-ordered ferromagnetic planes of LaMnO<sub>3</sub>, and show that it depends critically on the type of orbital ordering. While the hole does not couple to the spin excitations, it interacts strongly with the excitations of  $e_g$  orbitals (orbitons), leading to new types of quasiparticles with a dispersion on the orbiton energy scale and with strongly enhanced mass and reduced weight. Therefore we predict a large redistribution of spectral weight with respect to the bands found in local density approximation (LDA) or in LDA+U.

Transition metal (TM) compounds are well known for their large diversity and richness in phenomena [1]. This variety of properties is not only due to the strongly correlated nature of the electronic  $3d$  states in these systems, often rendering them magnetic, and to the strong hybridization with the extended ligand valence states, but also due to the orbital degeneracy of the open  $3d$  shells. In a localized system such orbital degeneracy will be lifted in one way or another – this is the well known Jahn-Teller (JT) effect. In concentrated systems this often leads to structural phase transitions accompanied by a certain ordering of occupied orbitals. Alternatively, strong correlations may lead to orbital order via superexchange interactions [2], which may dominate the JT related contribution [3]. Effects of this kind are observed in TM compounds with three-fold  $t_g$  orbital degeneracy, for example in LiVO<sub>2</sub> [4], but are strongest in compounds with a two-fold  $e_g$  orbital degeneracy, containing Mn<sup>3+</sup> or Cr<sup>2+</sup> ( $d^4$ ), Co<sup>2+</sup> or Ni<sup>3+</sup> ( $d^7$ ), or Cu<sup>2+</sup> ( $d^9$ ) ions in octahedral coordination. Some well-known examples are cubic (LaMnO<sub>3</sub>, KCrF<sub>3</sub> and KCuF<sub>3</sub>) and layered (LaSrMn<sub>2</sub>O<sub>7</sub> and K<sub>2</sub>CuF<sub>4</sub>) perovskites [2,5].

Superexchange interactions stabilize the magnetic and orbital order [6], and the low-energy excitations of the system are magnons and orbital waves (orbitons). For simplicity we shall neglect the coupling to JT phonons. In fact, it has been argued by Dagotto *et al.* [7] that if the Hund's rule interaction  $J_H$  is large, *the JT coupling leads to the same orbital pattern as superexchange*, and we assume that its effect can be absorbed in the renormalized parameters of the electronic model.

In this Letter we present a study of single hole motion in a ferromagnetic (FM) orbital-ordered plane. Due to strong correlations the hole motion is restricted by the magnetic order [8]. In the FM and orbital ordered state [9] the hole can move without disturbing the background due to the off-diagonal hopping between  $e_g$  orbitals, and is essentially predicted by the band structure theory using either the local density approximation (LDA), or its modification for the correlated oxides, the LDA+U method [10]. The picture that arises from the

present work is, however, quite different. In addition to free propagation, the hole motion may frustrate the orbital order, just as it does for the antiferromagnetic order in the  $t$ - $J$  model. As we show below, the interaction between the hole and the orbitals is so strong in the manganites that propagating holes are dressed with many orbital excitations and form *orbital polarons* that have large mass, small bandwidth and low quasiparticle (QP) weight [11].

*Ground state* – The ground state of LaMnO<sub>3</sub> is formed by FM layers which stagger along the  $c$ -direction, also known as A-type antiferromagnetic phase. As a consequence of the double-exchange [12] the motion along the  $c$ -axis is hindered and propagation of holes occurs only within the FM ( $a, b$ )-planes. Consider first the order of degenerate  $e_g$  orbitals induced by superexchange in a two-dimensional (2D) FM plane with one electron per site ( $n = 1$ ). The orbital degrees of freedom are most conveniently described by pseudospins:  $T_i^z = \frac{1}{2}\sigma_i^z$  and  $T_i^x = \frac{1}{2}\sigma_i^x$ , where  $\sigma_i^\alpha$  are Pauli matrices, and we label the orbital  $|x\rangle \equiv |x^2 - y^2\rangle$  and  $|z\rangle \equiv |3z^2 - r^2\rangle$  states by the pseudospin components:  $|\uparrow\rangle \equiv |x\rangle$  and  $|\downarrow\rangle \equiv |z\rangle$ . In the limit of large on-site Coulomb interaction  $U$ , the effective interaction between the orbital pseudospins is given by the superexchange  $J > 0$ , which involves the high-spin  ${}^6A_1$  excited states [13]. One finds

$$H_J = \frac{1}{2}J \sum_{\langle ij \rangle} \left[ T_i^z T_j^z + 3T_i^x T_j^x \mp \sqrt{3}(T_i^x T_j^z + T_i^z T_j^x) \right], \quad (1)$$

where  $\langle ij \rangle$  denotes a nearest neighbor pair, and the negative (positive) sign applies to a bond along the  $a(b)$ -axis. In the ground state the occupied  $e_g$  orbitals are staggered:  $|\mu\rangle = (|x\rangle + |z\rangle)/\sqrt{2}$  and  $|\nu\rangle = (|x\rangle - |z\rangle)/\sqrt{2}$  on  $A$  and  $B$  sublattice, respectively [15]. These orbitals define locally a new basis obtained from  $\{|x\rangle, |z\rangle\}$  orbitals by a rotation by the same angle on the two sublattices,  $\psi_A = \psi_B = \frac{\pi}{4}$  [16].

We write the kinetic energy for holes introduced in the orbital-ordered state in terms of this new orbital basis,

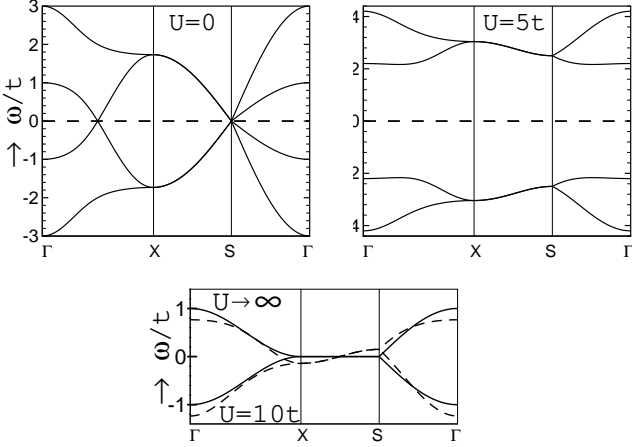


FIG. 1. Electronic structure in the reduced BZ [ $X = (\pi, 0)$ ,  $S = (\pi/2, \pi/2)$ ] as obtained from  $H_t$  (2) for:  $U = 0$  (left), and  $U = 5t$  (right). In the bottom part the lower Hubbard band (centered at  $\omega = 0$ ) obtained for  $U = 10t$  (dashed lines) is compared with the  $U \rightarrow \infty$  dispersion  $\varepsilon_{\mathbf{k}}^0(\phi = 0)$  (full lines).

$$H_t = \frac{1}{4}t \sum_{\langle ij \rangle} \left[ f_{i0}^\dagger f_{j0} + f_{i1}^\dagger f_{j1} + 2(f_{i1}^\dagger f_{j0} + f_{i0}^\dagger f_{j1}) \pm \sqrt{3} \left( f_{i1}^\dagger f_{j0} - f_{i0}^\dagger f_{j1} \right) + H.c. \right], \quad (2)$$

where  $f_{i\alpha}^\dagger$  creates a hole on site  $i$  in orbital  $\alpha$ , and upper (lower) sign applies to a bond  $\parallel a(b)$ -axis. Here the indices 0 and 1 refer to the occupied ( $|0\rangle$ ) and unoccupied ( $|1\rangle$ ) orbital states, as determined by  $H_J$ . The hopping integrals in Eq. (2) follow from the  $e_g$  symmetry and therefore depend strongly on the pair of orbitals at nearest-neighbor sites involved in a hopping process.

*LDA+U bands* – The Hamiltonian  $H_t$  gives a metallic system with a bandwidth of  $6t$ , and can be seen as a tight-binding representation of the  $e_g$  bands in an idealized structure without lattice distortions. However, LaMnO<sub>3</sub> is a Mott-Hubbard system with large on-site Coulomb repulsion  $U$  which acts between the *occupied* and *empty*  $e_g$  states,  $H_U = U \sum_i f_{i0}^\dagger f_{i0} f_{i1}^\dagger f_{i1}$ . In the orbital-ordered state at  $n = 1$  the charge fluctuations are suppressed and one may use the constraint  $f_{i0}^\dagger f_{i0} = 1$ . The Coulomb interaction acts then as a local potential on the unoccupied states, and the band structure is split into a lower and upper Hubbard band separated by a gap  $\propto U$ , as is typical for a Mott-Hubbard insulator (Fig. 1). For the manganites  $U/t \approx 10$ , and one finds that the lower Hubbard band has a dispersion  $\sim 2t$ , quite close to the  $U = \infty$  limit. This resembles the strong redistribution of the bands in the LDA+U approach with respect to those found within the LDA, as obtained for LaMnO<sub>3</sub> [17] when the local electron-electron interaction terms  $\propto U$  are treated in the mean-field approximation [18].

In our framework, however, the interpretation of Eq. (2) is quite different. On the site with the hole both

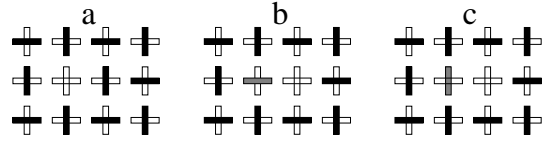


FIG. 2. Schematic representation of a hole in an orbital-ordered ground state (a). The occupied (empty) orbitals  $|\mu\rangle$  and  $|\nu\rangle$  are shown as filled (empty) rectangles. The hole can move either without disturbing the orbital order (b), or by creating orbital excitations (c).

orbitals are empty [Fig. 2(a)]. An electron on a neighboring site can hop to either one of these orbitals. If the orbital order is preserved in the hopping process [Fig. 2(b)], the hole propagates freely with a dispersion determined by the first term  $\sim f_{i0}^\dagger f_{j0}$  in  $H_t$ . Unlike in the  $t$ - $J$  model, the hopping couples the orthogonal states  $|\mu\rangle$  and  $|\nu\rangle$  on both sublattices. In contrast, if the orbital order is locally disturbed by the hopping process  $\sim f_{i1}^\dagger f_{j0}$  [Fig. 2(c)], an orbital excitation occurs [19]. In this way the propagation of the hole is coupled to the orbital excitations determined by  $H_J$ . This coupling is a direct consequence of the strongly correlated nature of the  $e_g$  electrons and its repercussions on the low energy electron dynamics cannot be taken into account within a mean-field (or LDA+U) treatment of the correlations.

*Orbital  $t$ - $J$  model* – Our total Hamiltonian,

$$\mathcal{H} = H_t + H_J + H_z, \quad (3)$$

includes, in addition to  $H_J$  (1) and  $H_t$  (2), a crystal-field term  $H_z = -E_z \sum_i T_i^z$ , which occurs, e.g., due to uniaxial pressure. It acts like a magnetic field in the orbital sector which modifies the occupied orbitals and implies *different* basis rotations by  $\psi_{A(B)} = \frac{\pi}{4} \mp \phi$  on  $A$  and  $B$  sublattice [16], respectively, with  $\sin 2\phi = -E_z/4J$ .

*Free hole dispersion* – The hopping of the hole can be expressed by the change of the orbital background using the Schwinger boson representation [20] for the orbital variables which obey the constraint of no double occupancy in the limit of  $U \rightarrow \infty$ :  $f_{i0}^\dagger = b_{i0} h_i^\dagger$  and  $f_{i1}^\dagger = b_{i1} h_i^\dagger$ , with  $h_i^\dagger$  standing for a moving fermionic hole. In the orbital ordered state the  $b_{i0}$  bosons are condensed,  $b_{i0} \simeq 1$ , which leads to a free dispersion of the hole (Fig. 1),

$$H_h = \sum_{\mathbf{k}} \varepsilon_{\mathbf{k}}^0(\phi) h_{\mathbf{k}}^\dagger h_{\mathbf{k}}, \quad (4)$$

where  $\varepsilon_{\mathbf{k}}^0(\phi) = t(-2 \sin 2\phi + 1)\gamma_{\mathbf{k}}$  is determined by the orbital order, and  $\gamma_{\mathbf{k}} = \frac{1}{2}(\cos k_x + \cos k_y)$ .

*Orbital excitations* – The orbital background is described by a local constraint for  $T = 1/2$  pseudospins  $b_{i0}^\dagger b_{i0} + b_{i1}^\dagger b_{i1} = 2T$ , where  $b_{i0}^\dagger$  and  $b_{i1}^\dagger$  are boson operators which refer to the occupied and empty state at site  $i$ . The orbital excitations are calculated by using the lowest-order expansion of the constraint around the orbital-ordered ground state:  $T_i^x \simeq \frac{1}{2}(b_i + b_i^\dagger)$  and  $T_i^z \simeq T - b_i^\dagger b_i$ ,

with  $b_i \equiv b_{i1}$ . The effective boson Hamiltonian is diagonalized by a Fourier and Bogoliubov transformation defined by  $b_{\mathbf{k}}^\dagger = u_{\mathbf{k}} \alpha_{\mathbf{k}}^\dagger + v_{\mathbf{k}} \alpha_{-\mathbf{k}}$ , with the coefficients  $\{u_{\mathbf{k}}, v_{\mathbf{k}}\}$  given in Ref. [16]. One finds

$$H_o = \sum_{\mathbf{k}} \omega_{\mathbf{k}}(\phi) \alpha_{\mathbf{k}}^\dagger \alpha_{\mathbf{k}}, \quad (5)$$

where  $\omega_{\mathbf{k}}(\phi) = 3J [1 + \frac{1}{3}(2 \cos 4\phi - 1)\gamma_{\mathbf{k}}]^{1/2}$  is the orbital dispersion. This single mode, defined in the full Brillouin zone (BZ), is equivalent to two branches of orbital excitations obtained in the folded zone in Ref. [16]. The orbital excitations depend sensitively on the orbital splitting  $E_z$ . At orbital degeneracy ( $E_z = 0$ ) one finds a maximum of  $\omega_{\mathbf{k}} = 3J(1 + \frac{1}{3}\gamma_{\mathbf{k}})^{1/2}$  at the  $\Gamma = (0, 0)$  point and a weak dispersion  $\sim J$ . In contrast, for  $E_z = \pm 2J$  orbital excitations are dispersionless, with  $\omega_{\mathbf{k}} = 3J$ .

*Hole-orbital coupling* – The remaining part of Eq. (2) describes the hole-orbital interaction [Fig. 2(c)],

$$H_{ho} = t \sum_{\mathbf{k}, \mathbf{q}} h_{\mathbf{k}+\mathbf{q}}^\dagger h_{\mathbf{k}} [M_{\mathbf{k}, \mathbf{q}} \alpha_{\mathbf{q}} + N_{\mathbf{k}, \mathbf{q}} \alpha_{\mathbf{q}+\mathbf{Q}} + H.c.], \quad (6)$$

where  $\mathbf{Q} = (\pi, \pi)$ ,  $M_{\mathbf{k}, \mathbf{q}} = 2 \cos 2\phi (u_{\mathbf{q}} \gamma_{\mathbf{k}-\mathbf{q}} + v_{\mathbf{q}} \gamma_{\mathbf{k}})$ ,  $N_{\mathbf{k}, \mathbf{q}} = -\sqrt{3} (u_{\mathbf{q}} \eta_{\mathbf{k}-\mathbf{q}} - v_{\mathbf{q}} \eta_{\mathbf{k}})$ , and  $\eta_{k_x, k_y} = \gamma_{k_x, k_y + \pi}$ . So far we have reduced the total Hamiltonian (3) to an effective Hamiltonian  $\mathcal{H}_{eff} = H_h + H_o + H_{ho}$ , linearized in the slave fermion formalism, and treating orbital and hole dynamics on equal footing. Let us, for clarity, summarize the differences to the standard  $t$ - $J$  model describing a hole in a quantum antiferromagnet: (i) the orbital model (3) contains a free dispersion of the hole  $\varepsilon_{\mathbf{k}}^0(\phi)$  which depends strongly on  $E_z$ ; (ii) the orbital excitations are in general different when the momentum is changed by a nesting vector  $\mathbf{Q}$  [ $\omega_{\mathbf{k}+\mathbf{Q}}(\phi) \neq \omega_{\mathbf{k}}(\phi)$ ], and their dispersion varies with  $E_z$ , and finally, (iii) the hole scattering on the orbital excitations has a richer analytic structure than in the  $t$ - $J$  model, with new processes  $\propto N_{\mathbf{k}, \mathbf{q}}$ . A qualitatively similar case to the  $t$ - $J$  model arises at  $E_z = -2J$ , where the free dispersion vanishes, but the orbital excitations are simultaneously dispersionless, so that the orbital model (3) reduces to the  $t$ - $J^z$  model.

We investigate the spectral function and QP properties using the self-consistent Born-approximation (SCBA) [21], known to be very reliable for the single hole problem [20]. Treating  $\mathcal{H}_{eff}$  in the SCBA, we find the selfenergy

$$\Sigma(\mathbf{k}, \omega) = t^2 \sum_{\mathbf{q}} [M_{\mathbf{k}, \mathbf{k}-\mathbf{q}}^2 G(\mathbf{k}-\mathbf{q}, \omega - \omega_{\mathbf{q}}(\phi)) + N_{\mathbf{k}, \mathbf{k}-\mathbf{q}}^2 G(\mathbf{k}-\mathbf{q}, \omega - \omega_{\mathbf{q}+\mathbf{Q}}(\phi))], \quad (7)$$

which, together with the Dyson equation for the hole Green function  $G(\mathbf{k}, \omega)$ , represents a closed set of equations and was solved self-consistently by numerical iteration on a grid using 160  $\mathbf{k}$ -points.

*Quasiparticles* – The spectral functions found in SCBA,  $A(\mathbf{k}, \omega) = -\frac{1}{\pi} \text{Im}G(\mathbf{k}, \omega)$ , consist of a QP band

FIG. 3. Contour plot of the spectral function (left) and density of states DOS (right, blue lines) for  $J/t = 0.2$ ,  $E_z = 0$  (top) and  $E_z = 2J$  (bottom). Quasiparticle states at the top of the valence band are highlighted in yellow color, while free hole bands  $\varepsilon_{\mathbf{k}}^0(\phi)$  and DOS are shown by red lines.

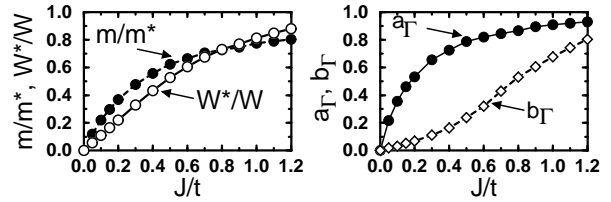


FIG. 4. Quasiparticle properties at  $E_z = 0$  as functions of  $J/t$ : (a) inverse effective mass  $m/m^*$  (full circles) and the bandwidth  $W^*/W$  (empty circles) in units of  $m$  and  $W$  defined by  $\varepsilon_{\mathbf{k}}^0(0)$  (4); (b) weights of high-energy QP  $a_{\Gamma}$  (filled circles) and low-energy QP  $b_{\Gamma}$  (open squares) at the  $\Gamma$  point.

close to the Fermi energy, while the excitations deep in the valence band are incoherent, taking typical values of  $J/t < 0.5$ . In Fig. 3 we present contour plots of the spectral function. The total width of the spectrum is comparable to the free dispersion, as shown by the density of states, but the coupling to the orbitals leads to a strong redistribution of spectral weight.

As the accurate orbital wave functions are not known [9], we investigated the spectra for a few representative orbital ordered states. The QP part of the spectral function obtained for the alternating  $(|x \pm |z|)/\sqrt{2}$  orbital order at  $E_z = 0$  resembles the free dispersion with a maximum at the  $\Gamma$  point, but its bandwidth is reduced to  $\sim J$ . When  $E_z = 2J$ , which corresponds to the alternation of  $3x^2 - r^2/3y^2 - r^2$  orbitals [22], the spectral function changes markedly (Fig. 3). The incoherent weight is now distributed more smoothly and the original free dispersion  $\varepsilon_{\mathbf{k}}^0(\phi)$  (red lines) can still be recognized in the spectral function but is strongly damped. Most strikingly, there is only one QP band with appreciable weight left in a limited region of the BZ, while the second band is absorbed by the continuum. In the opposite case of  $E_z = -2J$ , i.e.,  $x^2 - z^2/y^2 - z^2$  orbitals alternate, the spectrum (not shown) is identical to the *ladder spectrum* of the  $t$ - $J^z$  model; it is  $\mathbf{k}$ -independent and consists of a set of  $\delta$ -functions at approximately equal energy intervals [21]. In this respect the spectrum found at  $E_z = 0$  can be viewed as a compromise between the extremes of the ladder spectrum, from which it retains some character of the enhanced/reduced spectral weight at regular energy intervals, and the  $E_z = 2J$  spectrum in which the dispersive features are smeared out over the entire band.

Finally, we analyze the QP properties at orbital degeneracy ( $E_z = 0$ ). Two QP states at the  $\Gamma$  point have the spectral weights  $a_{\Gamma}$  and  $b_{\Gamma}$ , respectively, and determine the bandwidth  $W^*$  of the QP band (Fig. 4). At low doping the states at the top of the QP

band are filled by holes, and thus the transport properties depend on the effective mass found at the  $\Gamma$  point,  $(\partial^2 E_{\mathbf{k}}/\partial k^2)|_{\mathbf{k}=0} \propto m/m^*$ , where  $E_{\mathbf{k}}$  is the QP energy. In the weak-coupling regime ( $J > t/2$ ) the QP bandmass is almost unrenormalized, while it is strongly enhanced in the strong-coupling regime ( $J < t/2$ ). For the manganites  $J/t \simeq 0.1$  [14], so that  $W^*/W \simeq 0.1$ , and the QP mass  $m^*$  is *increased by an order of magnitude* due to the dressing of a hole by the orbital excitations. The weights of the two QP branches at the  $\Gamma$  point are strongly reduced in the strong-coupling regime, but the QP at the top of the valence band is still quite distinct.

*Summary* – In conclusion, we have shown that a hole moving in FM planes of  $\text{LaMnO}_3$  couples strongly to orbital excitations which results in a large redistribution of spectral weight compared to single-electron or mean-field treatments. The coherent quasiparticle band and the incoherent part of the spectral function depend critically on the orbital ordering and would therefore be *different* for FM planes of cubic and layered manganites. This prediction could be verified by angle resolved photoemission. Unfortunately, such experiments have not yet been performed in the orbital-ordered phase at low doping concentration. Recent experiments by Dessau *et al.* [23] on the highly doped layered system  $\text{La}_{1.2}\text{Sr}_{1.8}\text{Mn}_2\text{O}_7$  showed strong incoherent features which were discussed in terms of small lattice polarons. Our study points out that the incoherence observed in these experiments might be attributed instead to orbital excitations.

One of us (J.v.d.B.) acknowledges with appreciation the support by the Alexander von Humboldt-Stiftung, Germany. A.M.O. thanks the Committee of Scientific Research (KBN) Project No. 2 P03B 175 14 for support.

---

[1] M. Imada, A. Fujimori, and Y. Tokura, *Rev. Mod. Phys.* **70**, 1039 (1998).  
 [2] K. I. Kugel and D. I. Khomskii, *Usp. Fiz. Nauk* **136**, 621 (1982) [*Sov. Phys. Usp.* **25**, 231 (1982)]; A. M. Oleś, L. F. Feiner, and J. Zaanen, *Phys. Rev. B* **61**, 6257 (2000).  
 [3] P. Benedetti and R. Zeyher, *Phys. Rev. B* **59**, 9923 (1999).  
 [4] H. F. Pen *et al.*, *Phys. Rev. Lett.* **78**, 1323 (1997).  
 [5] G. A. Gehring and K. A. Gehring, *Rep. Prog. Phys.* **38**, 1 (1975).  
 [6] J. B. Goodenough, *Magnetism and Chemical Bond* (Interscience, New York, 1963).  
 [7] T. Hotta, A. L. Malvezzi, and E. Dagotto, *Phys. Rev. B* **62**, in press (2000).  
 [8] J. van den Brink and D. Khomskii, *Phys. Rev. Lett.* **82**, 1016 (1999); J. van den Brink, G. Khaliullin, and D. Khomskii, *ibid.* **83**, 5118 (1999).  
 [9] Y. Murakami *et al.*, *Phys. Rev. Lett.* **80**, 1932 (1998).

[10] V. I. Anisimov, J. Zaanen, and O. K. Andersen, *Phys. Rev. B* **44**, 943 (1991).  
 [11] The present orbital polaron is not coupled to the lattice; the electron-phonon coupling would further renormalize its mass and bandwidth [see also R. Kilian and G. Khaliullin, *Phys. Rev. B* **60**, 13 458 (1999)].  
 [12] C. Zener, *Phys. Rev.* **82**, 403 (1951); P. W. Anderson and H. Hasegawa, *Phys. Rev.* **100**, 675 (1955).  
 [13] L. F. Feiner and A. M. Oleś, *Phys. Rev. B* **59**, 3295 (1999).  
 [14] Taking realistic parameters of  $\text{LaMnO}_3$ , one finds (the effective)  $U \simeq 3.8$  eV for  $|{}^6A_1\rangle$  state which with  $t = 0.4$  eV gives  $J/t = t/U \simeq 0.1$  [13]. The same form of the effective interaction follows also from the cooperative JT effect which would enhance  $J$  by a factor close to two.  
 [15] Staggered orbital ordering follows also from the cooperative JT effect [A. J. Millis, *Phys. Rev. B* **53**, 8434 (1996)], and is most naturally explained by *strong* electron repulsion  $U$  and a rather *weak* electron-phonon coupling [3].  
 [16] J. van den Brink *et al.*, *Phys. Rev. B* **59**, 6795 (1999).  
 [17] S. Satpathy, Z. S. Popović, and F. R. Vukajlović, *Phys. Rev. Lett.* **76**, 960 (1996).  
 [18] A large Mott-Hubbard gap is obtained when the local correlations are included either in LDA+U [17] or in Hartree-Fock approximation [Y. S. Su *et al.*, *Phys. Rev. B* **61**, 1324 (2000)], while LDA gives only a small gap which opens due to the JT distortions [W. E. Pickett and D. Singh, *Phys. Rev. B* **53**, 1146 (1996)].  
 [19] Such processes lead to the string effect in the  $t$ - $J$  model; for a review see: E. Dagotto, *Rev. Mod. Phys.* **66**, 763 (1994).  
 [20] G. Martínez and P. Horsch, *Phys. Rev. B* **44**, 317 (1991).  
 [21] C. L. Kane, P. A. Lee, and N. Read, *Phys. Rev. B* **39**, 6880 (1989).  
 [22] In the present model this orbital order is induced by a finite value of  $E_z = 2J$ , while it could be also obtained taking an appropriately distorted lattice [T. Hotta *et al.*, *Phys. Rev. B* **60**, R15 009 (1999)].  
 [23] D. S. Dessau *et al.*, *Phys. Rev. Lett.* **81**, 192 (1998).

This figure "fig3.gif" is available in "gif" format from:

<http://arxiv.org/ps/cond-mat/0104496v1>